17. B. V. Deryagin and S. V. Nerpin, "Equilibrium, stability, and kinetics of free liquid films," Dokl. Akad. Nauk SSSR, 99, No. 6, 1029-1032 (1954).

NUMERICAL AND EXPERIMENTAL STUDY OF A NONISOTHERMAL TURBULENT JET WITH A HEAVY IMPURITY

L. B. Gavin, A. S. Mul'gi, and V. V. Shor

UDC 532.529

Temperature and momentum distributions of the carrier phase are determined experimentally and compared to results of numerical calculations using the (k − ε) model.

A second-order turbulence model using transfer equations for pulsation quantities was proposed in [1, 2] for calculation of two-phase jets. Experimental material permitting verification of models describing isothermal flows was presented in [3-5]. In connection with the wide use of nonisothermal two-phase turbulent jets in various equipment, the development of models for such flows and their experimental verification are a problem of very practical interest.

We will present below the results of an experimental and numerical study of a nonisothermal turbulent gas-suspension jet. A two-parameter turbulence model using transfer equations for pulsation energy and its dissipation rate is employed.

Mathematical Model. The system of equations describing escape of a nonisothermal two-phase turbulent isobaric axisymmetric submerged jet with consideration of velocity and temperature nonequilibrium between the phases, as obtained in the boundary-layer theory approximation, has the following form for the average values of the quantities:

$$\frac{\partial}{\partial x}(\rho_g u_g)+\frac{1}{y}\frac{\partial}{\partial y}(y\rho_g v_g)=0, \tag{1}$$

$$\frac{\partial}{\partial x}(\rho_p u_p)+\frac{1}{y}\frac{\partial}{\partial y}(y(\rho_p v_p+\langle \rho_p' v_p'\rangle))=0, \tag{2}$$

$$\rho_g\left(u_g\frac{\partial u_g}{\partial x}+v_g\frac{\partial u_g}{\partial y}\right)=\frac{1}{y}\frac{\partial}{\partial y}\left(y\rho_g\nu_t\frac{\partial u_g}{\partial y}\right)-F_x, \tag{3}$$

$$\rho_p u_p\frac{\partial u_p}{\partial x}+(\rho_p v_p+\langle \rho_p' v_p'\rangle)\frac{\partial u_p}{\partial y}+\frac{1}{y}\frac{\partial}{\partial y}(y\rho_p\langle u_p' v_p'\rangle)=F_x, \tag{4}$$

$$\rho_p u_p\frac{\partial v_p}{\partial x}+(\rho_p v_p+\langle \rho_p' v_p'\rangle)\frac{\partial v_p}{\partial y}+\frac{1}{y}\frac{\partial}{\partial y}(y(\rho_p\langle v_p'^2\rangle+v_p\langle \rho_p' v_p'\rangle))=F_y, \tag{5}$$

$$\rho_p u_p\frac{\partial \omega_{p\varphi}}{\partial x}+(\rho_p v_p+\langle \rho_p' v_p'\rangle)\frac{\partial \omega_{p\varphi}}{\partial y}+\frac{1}{y}\frac{\partial}{\partial y}(y\rho_p\langle v_p'\omega_{p\varphi}'\rangle)=-\rho_p\beta_\omega\Omega, \tag{6}$$

$$\rho_g\left(u_g\frac{\partial h_g}{\partial x}+v_g\frac{\partial h_g}{\partial y}\right)=\frac{1}{y}\frac{\partial}{\partial y}\left(y\lambda_t\frac{\partial T_g}{\partial y}\right)+$$
$$+\rho_g\nu_t\left(\frac{\partial u_g}{\partial y}\right)^2-Q_{gp}+F_x(u_g-u_p)+F_y(v_g-v_p), \tag{7}$$

Kaliningrad Fishing and Farm Industry Technical Institute. Thermophysics and Electrophysics Institute, Academy of Sciences of the Estonian SSR, Tallin. Translated from Inzhenerno-Fizicheskii Zhurnal, Vol. 50, No. 5, pp. 735-743, May, 1986. Original article submitted April 30, 1985.

0022-0841/86/5005-0505$12.50

$$\rho_p u_p \frac{\partial h_p}{\partial x} + (\rho_p v_p + \langle \rho_p' v_p' \rangle) \frac{\partial h_p}{\partial y} + \frac{1}{y} \frac{1}{\partial y} (y \rho_p \langle h_p' v_p' \rangle) = Q_{gp}, \tag{8}$$

$$p = \rho_g R_g T_g, \tag{9}$$

$$\rho_g \left(u_g \frac{\partial k}{\partial x} + v_g \frac{\partial k}{\partial y} \right) = \frac{1}{y} \frac{\partial}{\partial y} \left(y \rho_g \frac{\nu_t}{\sigma_k} \frac{\partial k}{\partial y} \right) + \tag{10}$$

$$+ \rho_g \left(\nu_t \left(\frac{\partial u_g}{\partial y} \right)^2 - \varepsilon - \varepsilon_p \right),$$

$$\rho_g \left(u_g \frac{\partial \varepsilon}{\partial x} + v_g \frac{\partial \varepsilon}{\partial y} \right) = \frac{1}{y} \frac{\partial}{\partial y} \left(y \rho_g \frac{\nu_t}{\sigma_\varepsilon} \frac{\partial \varepsilon}{\partial y} \right) +$$

$$+ \rho_g \left(c_{\varepsilon 1} \frac{\varepsilon}{k} \nu_t \left(\frac{\partial u_g}{\partial y} \right)^2 - c_{\varepsilon 2} \frac{\varepsilon^2}{k} + c_{\varepsilon 3} \frac{\varepsilon^2}{k} \chi - \Phi_p \right), \tag{11}$$

$$\nu_t = c_\mu k^2/\varepsilon, \quad \lambda_t = c_g \rho_g \nu_t / \mathrm{Pr}_t,$$

$$\chi = -\frac{1}{4} \left(\frac{k}{\varepsilon} \right)^3 \left(\frac{\partial u_g}{\partial y} \right)^2 \left(\frac{\partial u_g}{\partial x} + \frac{\partial v_g}{\partial y} \right), \quad \langle \rho_p' v_p' \rangle = -D_p \frac{\partial \rho_p}{\partial y},$$

$$\varepsilon_p = \frac{1}{\rho_g} \sum_i \langle F_i' V_{gi}' \rangle, \quad \Phi_p = \frac{2\nu}{\rho_g} \sum_{ij} \left\langle \frac{\partial F_i'}{\partial x_j} \frac{\partial V_{gi}'}{\partial x_j} \right\rangle.$$

Correlations of gas parameter pulsations are represented in gradient form in the system of equations

$$\langle u_g' v_g' \rangle = -\nu_t \frac{\partial u_g}{\partial y}, \quad \rho_g \langle h_g' v_g' \rangle = -\lambda_t \frac{\partial T_g}{\partial y}.$$

In Eq. (6), in analogy to [1], the correlation $\langle \rho_p', \omega_p' \rangle$ is omitted since it is not yet possible to model it, while in Eq. (7) the correlations of velocity pulsations and interphase interaction forces are omitted because their contribution to the balance of the terms in the flow regimes considered is small in comparison to the contribution of other terms of the equation.

The dynamic interaction of the phases in the jet is defined essentially by the resistance force $\mathbf{F}_\mu$ and the Magnus force $\mathbf{F}_m$

$$\mathbf{F}_\mu^* = 0.75 c_f |\mathbf{V}_r^*| \mathbf{V}_r^* \rho_p^* \rho_g^{\circ *} / (\rho_p^\circ \delta), \quad \mathbf{V}_r^* = \mathbf{V}_g^* - \mathbf{V}_p^*, \tag{12}$$

$$\mathbf{F}_m^* = c_m \mathbf{V}_r^* \times (\omega_p^* - 0.5 \mathrm{rot}\, \mathbf{V}_g^*) \rho_g^{\circ *} \rho_p^* / \rho_p^\circ, \tag{13}$$

where the resistance coefficient of a spherical particle is described by the standard resistance curve

$$c_f = \frac{24}{\mathrm{Re}_p^*} (1 + b_1 \mathrm{Re}_p^{*1/2} + b_2 \mathrm{Re}_p^*); \quad \mathrm{Re}_p^* = \frac{\delta |\mathbf{V}_r^*|}{\nu^*};$$

$b_1 = 0.179$, $b_2 = 0.013$, and the coefficient c_m for high numbers $\mathrm{Re}_\omega = \delta^2 |\omega_p| / \nu$ is equal to two, as was shown in [6]. The molecular viscosity coefficient of air ν as a function of temperature was calculated by Sutterland's expression [7]. It was assumed that thermal interaction between phases is defined by the expresion [6]

$$Q_{gp} = 6 \mathrm{Nu} \lambda (T_g - T_p) \rho_p / (\rho_p^\circ \delta^2). \tag{14}$$

The particle turbulent diffusion coefficient D_p was found using the theory of [8]. Determination of the additional dissipative terms ε_p and Φ_p and the correlations of pulsation velocities and temperatures of the dispersed phase were performed with consideration of flow inhomogeneity [9, 10]. To find these values we use the equations of conservation of momentum and energy [11], together with the equation of conservation of the moment of momentum of the dispersed phase:

$$\frac{\partial V_{pi}^*}{\partial t} + V_{pj}^* \frac{\partial V_{pi}^*}{\partial x_j} = \frac{F_i^*}{\rho_p^*}, \quad \frac{\partial \omega_{p\varphi}^*}{\partial t} + V_{pj}^* \frac{\partial \omega_{p\varphi}^*}{\partial x_j} = -\beta_\omega^* \Omega^*, \tag{15}$$

$$\frac{\partial T_p^*}{\partial t} + V_{pj}^* \frac{\partial T_p^*}{\partial x_j} = \frac{Q_{gp}^*}{c_p^* \rho_p^*}. \tag{15}$$

Representing all parameters in Eq. (15) in the form of the sum of average and pulsation components, and subtracting from the equations for the instantaneous values the corresponding equations for the averaged values and neglecting the squares of pulsations, we obtain equations for the Euler pulsation velocities and temperature in integral form at the point r(x, y):

$$u_p'(r,\ t) = u_p'(r,\ 0)\exp(-\gamma_{xx}t) + \int_0^t \exp(-\gamma_{xx}(t-\tau))\left[\gamma_{xx}^{\circ} u_g'(r,\ \tau) + \gamma_{xy}^{\circ} v_g'(r,\ \tau) - \gamma_{xy} v_p'(r,\ \tau) + \right. \tag{16}$$

$$\left. + \lambda_\omega v_r \Omega'(r,\ \tau) - u_p \frac{\partial u_p'(r,\ \tau)}{\partial x} - v_p \frac{\partial u_p'(r,\ \tau)}{\partial y}\right] d\tau,$$

$$v_p'(r,\ t) = v_p'(r,\ 0)\exp(-\gamma_{yy}t) + \int_0^t \exp(-\gamma_{yy}(t-\tau))\left[\gamma_{yy}^{\circ} v_g'(r,\ \tau) + \gamma_{yx}^{\circ} u_g'(r,\ \tau) - \gamma_{yx} u_p'(r,\ \tau) - \right.$$

$$\left. - \lambda_\omega u_r \Omega'(r,\ \tau) - u_p \frac{\partial v_p'(r,\ \tau)}{\partial x} - v_p \frac{\partial v_p'(r,\ \tau)}{\partial y}\right] d\tau, \tag{17}$$

$$\omega_{p\varphi}'(r,\ t) = \omega_{p\varphi}'(r,\ 0)\exp(-\beta_\omega t) - \int_0^t \exp(-\beta_\omega(t-\tau))\times$$

$$\times\left[0.5\beta_\omega \frac{\partial u_g'(r,\ \tau)}{\partial y} + u_p \frac{\partial \omega_{p\varphi}'(r,\ \tau)}{\partial x} + v_p \frac{\partial \omega_{p\varphi}'(r,\ \tau)}{\partial y} + \right.$$

$$\left. + u_p'(r,\ \tau)\frac{\partial \omega_{p\varphi}}{\partial x} + v_p'(r,\ \tau)\frac{\partial \omega_{p\varphi}}{\partial y}\right] d\tau, \tag{18}$$

$$T_p'(r,\ t) = T_p'(r,\ 0)\exp(-\theta t) + \int_0^t \exp\ (-\theta(t-\tau))\left[\theta T_g'(r,\ \tau) - \right.$$

$$\left. - u_p'(r,\ \tau)\frac{\partial T_p}{\partial x} - v_p'(r,\ \tau)\frac{\partial T_p}{\partial y} - u_p \frac{\partial T_p'(r,\ \tau)}{\partial x} - v_p \frac{\partial T_p'(r,\ \tau)}{\partial y}\right] d\tau, \tag{19}$$

$$\gamma_{ii} = \gamma_{ii}^{\circ} + \partial V_{pi}/\partial x_i,\ \gamma_{ij} = \gamma_{ij}^{\circ} + \partial V_{pi}/\partial x_j,$$

$$\gamma_{ii}^{\circ} = \gamma + \gamma_0 V_{ri}^2/V_r^2,\ \gamma_{ij}^{\circ} = \gamma_0 V_{ri} V_{rj}/V_r^2 + (-1)^{\delta_{iy}}\lambda_\omega \Omega,$$

$$\gamma = \beta(1 + b_1 \mathrm{Re}_p^{1/2} + b_2 \mathrm{Re}_p),\ \gamma_0 = \beta\left(\frac{1}{2} b_1 \mathrm{Re}_p^{1/2} + b_2 \mathrm{Re}_p\right),$$

$$\beta = \frac{18\rho_g^{\circ}\nu}{\rho_p^{\circ}\delta^2},\ \beta_\omega = \frac{10}{3}\beta,\ \theta = \frac{6\lambda \mathrm{Nu}}{\rho_p^{\circ} c_p \delta^2},\ \lambda_\omega = \frac{c_m \rho_g^{\circ}}{\rho_p^{\circ}}.$$

Multiplying Eqs. (16)-(19) by the corresponding pulsation values and averaging, we find all the Euler time correlations needed to complete system (1)-(11) with consideration of flow inhomogeneity. For example, for the correlation moments <up'(r, t)vp'(r, t)>, <Tp'(r, t)·vp'(r, t)> we have expressions

$$\langle u_p' v_p' \rangle = \frac{(\gamma_{xx}^{\circ}\gamma_{yy}^{\circ} + \gamma_{xy}^{\circ}\gamma_{yx}^{\circ})(\gamma_{xx} + 2\varphi_{xy} + \gamma_{yy})}{(\gamma_{xx} + \gamma_{yy})(\gamma_{xx} + \varphi_{xy})(\gamma_{yy} + \varphi_{xy})} \langle u_g' v_g' \rangle + \tag{20}$$

$$+ \frac{2k}{3(\gamma_{xx} + \gamma_{yy})}\left[\frac{\gamma_{yy}^{\circ}\gamma_{xy}^{\circ}(\gamma_{xx} + 2\varphi_{yy} + \gamma_{yy})}{(\gamma_{xx} + \varphi_{yy})(\gamma_{yy} + \varphi_{yy})} + \frac{\gamma_{xx}^{\circ}\gamma_{yx}^{\circ}(\gamma_{xx} + 2\varphi_{xx} + \gamma_{yy})}{(\gamma_{xx} + \varphi_{xx})(\gamma_{yy} + \varphi_{xx})}\right],$$

$$\langle T_p' v_p' \rangle = \frac{\theta(\gamma_{yy} + 2a_t + \theta)}{(\gamma_{yy} + \theta)(\gamma_{yy} + a_t)(\theta + a_t)}(\gamma_{yy}^{\circ}\langle T_g' v_g' \rangle + \gamma_{yx}^{\circ}\langle T_g' u_g' \rangle). \tag{21}$$

In deriving Eqs. (20), (21) the following approximations of Euler time correlations of velocity and temperature of the carrier phase were used:

$$\langle V'_{gi}(r, t)V'_{gj}(r, t+\tau)\rangle = \langle V'_{gi}(r, t)V'_{gj}(r, t)\rangle \exp(-\varphi_{ij}\tau),$$

$$\langle T'_g(r, t)V'_{gi}(r, t+\tau)\rangle = \langle T'_g(r, t)V'_{gi}(r, t)\rangle \exp(-a_{ti}\tau),$$

$$\varphi_{xx} = T_E^{-1},\ T_E = \Lambda_E/u_g,\ \Lambda_E = c_t k^{3/2}/\varepsilon,$$

$$\varphi_{xy} = \xi_2\varphi_{yy},\ a_t = a_{ti} = \xi_1\varphi_{yy}.$$

Determination of the decrement of the transverse Euler time correlation function φ_{yy} is beset with significant difficulties. However, φ_{yy} can be determined in terms of φ_{xx} from the relationships for the Euler spatial correlations [12] Ryy = Rxx + 0.5xdRxx/dx, which are known for isotropic turbulence in an incompressible liquid. With use of the Taylor hypothesis x = $u_g\tau$, we obtain $\varphi_{yy}=2\varphi_{xx}$.

The boundary conditions for system (1)-(11) have the form

$$y = 0:\ \frac{\partial u_g}{\partial y} = \frac{\partial u_p}{\partial y} = \frac{\partial \rho_p}{\partial y} = \frac{\partial h_g}{\partial y} = \frac{\partial h_p}{\partial y} =$$

$$= \frac{\partial k}{\partial y} = \frac{\partial \varepsilon}{\partial y} = v_g = v_p = \omega_{p\varphi} = 0;$$

$$y = \infty:\ u_g = u_p = \rho_p = k = \varepsilon = 0,\ T_g = T_p = T_s,\ \frac{\partial v_p}{\partial y} = \frac{\partial \omega_{p\varphi}}{\partial y} = 0;$$

$$x = 0:\ u_g = u_{g0}(y),\ u_p = u_{p0}(y),\ v_p = v_{p0}(y),\ \rho_p = \rho_{p0}(y),$$

$$\omega_{p\varphi} = \omega_{p\varphi 0}(y),\ T_g = T_{g0}(y),\ T_p = T_{p0}(y),\ k = k_0(y),\ \varepsilon = \varepsilon_0(y).$$

The system of equations with these boundary conditions was solved numerically by the finite difference method using an implicit six-point scheme [13]. Error in the calculations was monitored by testing the fulfillment of the laws of conservation of dispersed phase flow rate, total excess jet momentum, and excess heat flux, which varied no more than 1%. The generally accepted empirical constants of [14] were used: c_μ = 0.09, σ_k = 1.0, σ_ε = 1.3, $c_{\varepsilon 1}$ = 1.45, $c_{\varepsilon 2}$ = 1.90, $c_{\varepsilon 3}$ = 0.79. The turbulent Prandtl number Pr_t = 0.86. The empirical constant c_t and coefficients ξ_1, ξ_2 were taken equal to 0.2, 1, 1, respectively.

Experimental Equipment and Measurement Technique. A two-phase nonisothermal flow escaping into a submerged space was formed in a 3-m long horizontal tube with a diameter of 0.016 m. Air was supplied from a compressor, and dispersed material in the form of Al_2O_3 micropowder with true density ρ_p° = 3960 kg/m³ was introduced through a special worm feed which allowed maintenance of the solid phase flow rate within the limits G = 0-0.05 kg/sec to an accuracy of 2%. The experimental tube itself was used as the heater element, with electric current up to 1300 A passed through the wall. Current was regulated by a thyristor regulator, permitting application of power levels up to 13 kW to the tube. The maximum temperature head of the two-phase mixture at a flow concentration of $\varkappa = G_p/G_g$ = 1.5 kg/kg reached 800°K. Car-

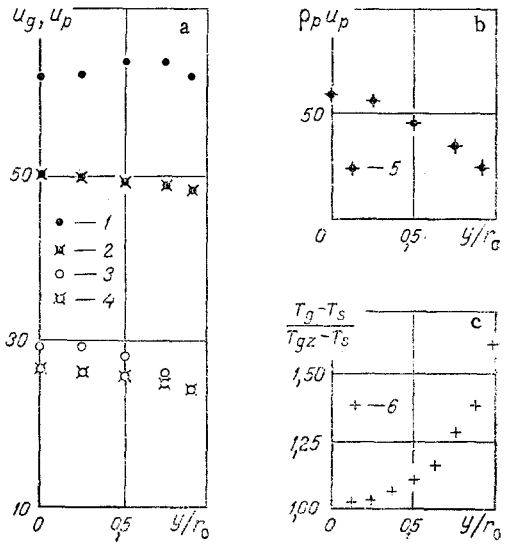

Fig. 1. Initial conditions: a) gas (1, 3) and particle (2, 4) velocity profiles; b) impurity mass flow distribution; c) relative excess temperature profile: 1, 2, 5, 6) T_{gz}/T_s = 2.36; 3, 4) T_{gz}/T_s = 1, T_s = 291°K. u_g, u_p, m/sec; $\rho_p u_p$, kg/(m²·sec).

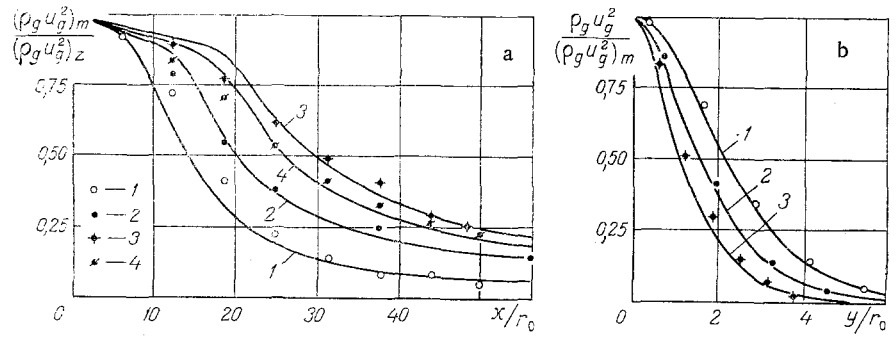

Fig. 2. Distribution of relative gas phase momenta along tube axis (a) and over cross section at $x = r_0 = 37.5$ (b): 1, 2) $T_{gz}/T_s = 2.36$; 3, 4) 1; 1) $\varkappa = 0$; 2) 1.41; 3) 1.52; 4) 1.11.

rier phase temperature was measured by Chromel–Copel thermocouples. Impurity mass flux density and momentum of the gas phase were determined by an isokinetic sampling tube [15], with collector section made of the solid alloy VK-6 and output orifice diameter of 0.0016 m. Components of the tube were silver soldered together for improved operation at high concentrations of the abrasive dispersed phase and high temperature. The experimental apparatus allowed generation of a steady-state two-phase nonisothermal jet and measurement of dynamic and thermal parameters of the flow at the exit from the tube and within the volume of the jet.

Results of Numerical and Experimental studies. Figure 1 shows the escape conditions found in experiments with particles $\delta = 5 \cdot 10^{-5}$ m in diameter for isothermal and nonisothermal cases. There is a marked velocity slippage of the phases: in the isothermal flow at $u_{gm} = 29.3$ m/sec the solid phase velocity $u_{pm} = 26.5$ m/sec ($u_{pm}/u_{gm} = 0.90$), while in the nonisothermal flow at $u_{gm} = 63.5$ m/sec the particle velocity $u_{pm} = 50$ m/sec ($u_{pm}/u_{gm} = 0.79$). The impurity mass flow densities coincide for the two cases.

To perform the numerical study it is also necessary to know the quantities $T_{p0}(y)$, $v_{p0}(y)$, $\omega_{p\varphi 0}(y)$, $k_0(y)$, $\varepsilon_0(y)$ in the initial section of the jet. Preliminary analytical calculations show that there is temperature inequality between the phases at the tube output, such that $T_{p0}(y) = 0.8T_{g0}(y)$. This result was used in the calculations. Transverse particle velocity was set equal to zero. Due to the lack of experimental data on $\omega_{p\varphi 0}(y)$, $k_0(y)$, $\varepsilon_0(y)$ the angular velocity of particle rotation was chosen to make the calculation results coincide with the experimental data on distribution of a dispersed impurity of similar coarseness in an isothermal jet [1], and the pulsation energy and its dissipation rate were determined by solution of the transfer equations for k and ε, describing the two-phase flow in the stabilized segment of the tube [16].

Figure 2 shows the change in gas phase momentum in isothermal and nonisothermal jets (here and below solid lines represent calculation results). It is evident that in the nonisothermal case drop in axial momentum occurs more rapidly in a single-phase jet than in a two-phase jet, due to the presence of momentum exchange between the phases. Upon escape of a jet with a dispersed impurity, attenuation of axial momentum occurs more intensely in the nonisothermal case than in the isothermal case at similar concentrations. The major cause of this is the following. In the transfer equations for $\varphi = (u_g, k, \varepsilon)$ in the nonisothermal case, aside from the term $\frac{1}{y}\frac{\partial}{\partial y}\left(y\nu_t\frac{\partial \varphi}{\partial y}\right)$ describing diffusion of the corresponding quantities in the isothermal case, there is a second term $\nu_t/\rho_g(\partial\rho_g/\partial y)(\partial\varphi/\partial y)$. In the case of positive superheating this term encourages more intense transfer of momentum in the transverse direction, which leads to more rapid attenuation of the longitudinal gas velocity along the jet axis. This also encourages an increase in turbulent viscosity along the jet axis due to intensification of diffusion of turbulent energy and its dissipation rate in the direction of the axis. Thus, scattering of momentum in the two-phase jet occurs more rapidly in the nonisothermal case than in the isothermal one, and most intensely of all in a single-phase heated jet (Fig. 2b).

Study of the heat-transfer process shows (Fig. 3) that the drop in axial excess gas temperature in a single-phase jet occurs more rapidly than in a two-phase jet with the same initial superheating, which can be explained by the presence of interphase heat exchange.

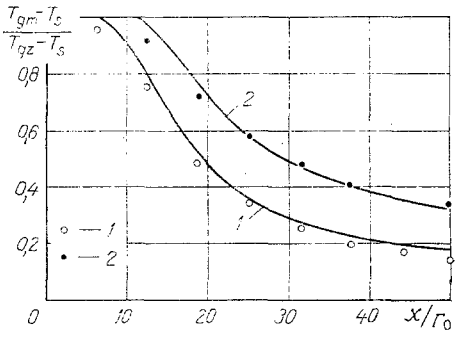

Fig. 3

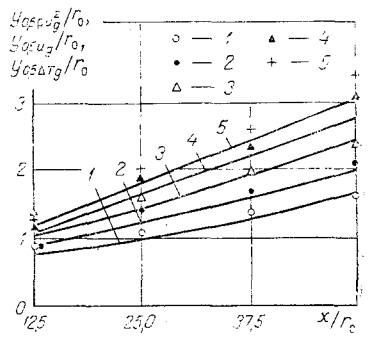

Fig. 4

Fig. 3. Distribution of axial excess gas temperature: T_{gz}/T_s = 2.36, 1) $\varkappa$ = 0; 2) 1.41.

Fig. 4. Jet boundaries at half-momentum level (1, 2), half-velocity (3, 4), half-excess temperature (5): 1, 3) T_{gz}/T_s = 1; 2, 4, 5) 2.36.

In the initial segment the particle temperature rapidly reaches the gas temperature, and in the main segment, due to their greater thermal inertia, the particles cool more slowly than the gas, transferring heat to the latter by interphase heat exchange.

It follows from Fig. 4 that expansion of the nonisothermal jet occurs more intensely.

As is evident from Figs. 2-4, the experimentally obtained results agree satisfactorily with the numerical results obtained by the proposed model

NOTATION

x, y, longitudinal and transverse coordinates; u, v, V_i, projections of average velocity onto x, y, i axes; ρ, ρ°, distributed and true densities; h, enthalpy; T, temperature; k, ε, kinetic energy of turbulent pulsations and its dissipation rate; ν, ν_t, λ, λ_t, coefficients of molecular and turbulent kinematic viscosity and thermal conductivity of gas; c_g, c_p, specific heats of gas and particles at constant pressure; p, gas pressure; R_g, gas constant; $\omega_{p\varphi}$, projection of particle rotation angular velocity vector on axis perpendicular to plane xy; $\Omega = \omega_{p\varphi} + 0.5\partial u_g/\partial y$, relative angular velocity; D_p, transverse particle diffusion coefficient; δ, particle diameter; r_0, tube radius; G, flow rate; F_μ, viscous resistance force; F_m, Magnus force; Re, Nu, Pr, Reynolds, Nusselt, and Prandtl numbers; Q_{gp}, interphase heat-exchange intensity; χ, dimensionless vortex deformation rate; t, τ, time; T_E, Λ_E, Euler time and space scales; R_{ij}, correlation coefficients; φ_{ij}, a_{ti} Euler time correlation exponents; γ_{ij}, coefficient; β, β_ω, θ, quantities inversely proportional to particle translational, rotational, and thermal relaxation times; δ_{ij}, Kronecker symbol; c_μ, σ_k, σ_ε, $c_{\varepsilon 1}$, $c_{\varepsilon 2}$, $c_{\varepsilon 3}$, empirical constants. Symbols with subscripts g, p indicate gas and particle parameters; z denotes flow in initial section on jet axis (x = 0, y = 0); 0, initial section (x = 0); m, on jet axis (y = 0); s, in submerged space (y = ∞); i, j, parameters referring to axes i and j; *, instantaneous, and ', pulsation values of parameters.

LITERATURE CITED

1. L. B. Gavin, V. A. Naumov, and V. V. Shor, "The k–ε model for a two-phase turbulent jet and its numerical study," in: Physicochemical Processes in Energy Equipment [in Russian], ITMO Akad. Nauk BSSR, Minsk (1983), pp. 11-15.
2. L. B. Gavin and V. A. Naumov, "Effect of a dispersed impurity on turbulent structure of a jet," Dokl. Akad. Nauk SSSR, 283, No. 2, 336-339 (1985).
3. M. K. Laats and F. A. Frishman, "Assumptions used in calculation of a two-phase jet," Izv. Akad. Nauk SSSR, Mekh. Zhidk. Gaza, No. 2, 186-191 (1970).
4. M. K. Laats and F. A. Frishman, "Study of turbulence intensity on the axis of a two-phase turbulent jet," Izv. Akad. Nauk SSSR, Mekh. Zhidk. Gaza, No. 2, 153-157 (1973).
5. T. A. Girshovich, A. I. Kartushinskii, M. K. Laats, et al., "Experimental study of a turbulent jet carrying a heavy impurity," Izv. Akad. Nauk SSSR, Mekh. Zhidk. Gaza, No. 5, 26-31 (1981).
6. R. I. Nigmatulin, Fundamentals of the Mechanics of Heterogeneous Media [in Russian], Nauka, Moscow (1978).

7. L. G. Loitsyanskii, Liquid and Gas Mechanics [in Russian], Nauka, Moscow (1978).
8. A. A. Shraiber, V. M. Milyutin, and V. P. Yatsenko, Hydrodynamics of Two-Component Flows with a Solid Polydispersed Material [in Russian], Naukova Dumka, Kiev (1980).
9. L. B. Gavin, "Modeling of turbulent gas flow in inhomogeneous shear flows," in: Turbulent Transfer Processes [in Russian], ITMO Akad. Nauk BSSR, Minsk (1985), pp. 89-101.
10. L. V. Kondrat'ev and V. V. Shor, "A model of a nonisothermal two-phase turbulent jet," in: Turbulent Transfer Processes [in Russian], ITMO Akad. Nauk BSSR, Minsk (1985), pp. 102-110.
11. I. V. Derevich, V. M. Eroshenko, and L. I. Zaichik, "Calculation of momentum and heat transfer in turbulent flow of a gas suspension in tubes," in: Heat–Mass Exchange VII, Vol. V, Pt. 1, Heat–Mass Exchange in Dispersed Systems [in Russian], ITMO Akad. Nauk BSSR (1984), pp. 141-146.
12. J. O. Hinze, Turbulence, McGraw-Hill (1960).
13. A. L. Dorfman and V. A. Maev, "Numerical modeling of viscous liquid jet flows," Inzh.-Fiz. Zh., 31, No. 4, 691-697 (1976).
14. S. B. Poup, "Explanation of the anomalous difference between propagation of axisymmetric and planar turbulent jets," Raketn. Tekh. Kosmonavt., 16, No. 3, 109-111 (1978).
15. M. K. Laats and F. A. Frishman, "Turbulent transfer processes in a two-phase jet," in: Transfer Processes in Flows with Shear [in Russian], ITÉF Akad. Nauk ESSR, Tallin (1973), pp. 104-199.
16. L. B. Gavin and V. V. Shor, "Numerical study of two-phase turbulent flows in a circular tube with escaping jet," in: Convective Heat Exchange and Hydrodynamics [in Russian], Naukova Dumka, Kiev (1985), pp. 128-132.

ANALYSIS OF LIQUID DROPLET DEFORMATION IN A GAS FLOW

V. V. Voronin

UDC 532.529.6:541.18.053

The small perturbation method is used to obtain equations describing the dynamics of a liquid droplet in a flow of ideal incompressible gas. The stability criteria and droplet disintegration time are determined.

The principles of motion of a liquid droplet in a gas flow with some relative velocity are of great practical interest and have been actively studied for several decades. The present state of studies of liquid droplet interaction with a carrier flow is presented quite fully in the review [1]. In particular, analysis of numerous experimental data has established a qualitative classification of the main types of droplet disintegration in a gas flow, which develops upon increase of the Weber number We; at We $\lesssim$ 100 droplet breakup is preceded by a "parachute"-type deformation which can be described within the framework of the approximate theory of flow over a deformed body.

Linearization of the defining equations establishes that a droplet in a gas flow spreads in the transverse direction with the form of the flattened droplet being close to an ellipsoid of rotation. Spreading of the droplet, which is maintained in the process of deformation of the ellipsoid form, was studied in detail in a number of works [2-5], in which simple asymptotes were obtained for the transverse deformation together with stability criteria for the droplet.

An analytical method for calculation of nonsteady-state motion and spreading of plane and axisymmetric drops of a viscous liquid in a gas flow was developed in [6]. This method is based on expansion of the Navier–Stokes equation in a small parameter, while the boundary problem is reduced to solution of an infinite system of differential equations with constant coefficients. In the absence of viscosity the system contains a finite number of equations

Translated from Inzhenerno-Fizicheskii Zhurnal, Vol. 50, No. 5, pp. 743-748, May, 1986. Original article submitted March 4, 1985.

0022-0841/86/5005-0511$12.50